

## **ACCELERATED DEGRADATION OF LI-ION BATTERIES FOR HIGH RATE DISCHARGE APPLICATIONS**

**Tony Thampan<sup>1</sup>, PhD, Yi Ding<sup>1</sup>, PhD, Laurence Toomey<sup>1</sup>, PhD, Alex Hundich<sup>1</sup>,  
Venkatesh Babu<sup>1</sup>**

<sup>1</sup>Combat Capabilities Development Command (CCDC), Ground Vehicle Systems  
Center (GVSC), Warren, MI

### **ABSTRACT**

*The U.S. Army has been pursuing vehicle electrification to achieve enhanced combat effectiveness. The benefits include supporting new capabilities that require high power pulse duty-cycles. These pulse power discharge rate can be significantly higher than commercial Hybrid Electric Vehicle (HEV) Energy Storage Systems (ESS) systems, resulting in significantly lower lifetimes than commercial applications. Results of high power pulse duty cycles on lifetime performance are presented as well as a discussion on the cause of degradation.*

**Citation:** T. Thampan, Y. Ding, L.Toomey, A. Hundich, V. Babu, “Accelerated degradation of Li-ion Batteries for High Rate Discharge Applications”, In *Proceedings of the Ground Vehicle Systems Engineering and Technology Symposium (GVSETS)*, NDIA, Novi, MI, Aug. 13-15, 2019.

### **1. INTRODUCTION**

The U.S. Army has been pursuing vehicle electrification to achieve enhanced combat effectiveness. The benefits of vehicle electrification via hybridization with Energy Storage Systems (ESS) include significant fuel savings / range extension, increased silent watch/mobility and new capabilities in Electronic Warfare (EW), High Power Sensors and Directed Energy (DE) systems<sup>1</sup>.

The discharge rates for silent mobility, a 30 kW DE and 100 kW DE capability using a Hybrid Electric Vehicle (HEV) configuration are shown in

Figure 1, along with examples of commercial systems. Note: Standard industry practice is to define charging / discharging by C rates. By definition a 1 C rate discharge is equivalent to a discharge current will discharge the entire battery in 1 hour.

The silent mobility power requirements has been normalized for combat vehicle platform weight (3.9kW/t) and the battery pack is proportionally sized (0.6 kWh/t). Thus the discharge rate for the silent mobility capability is constant across different platform sizes. This discharge rate can be met using existing HEV ESS solutions<sup>2</sup>. However, as the platform size decreases, the ESS discharge rates for DE capabilities increases significantly beyond standard HEV ESS solutions. In these

pulse power applications, the high power pulse duty-cycles<sup>3</sup> can have discharge rates that are significantly higher ( $> 10C$ ) than commercial HEV ESS systems, resulting in increased thermal and electrical stress.

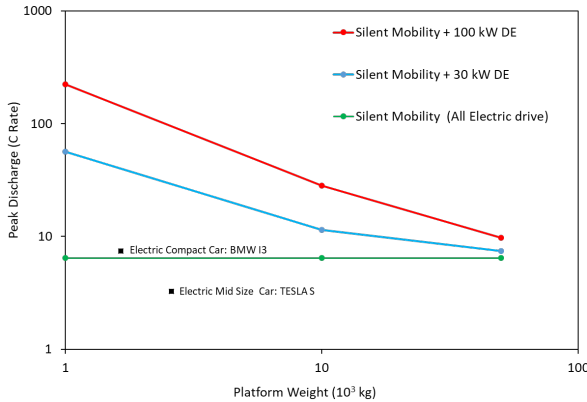


Figure 1: Battery capacity normalized with platform size to provide silent mobility and directed energy capabilities

## 2. Previous Work

There has been limited published experimental work on high rate discharge. However, Wong et al. tested  $\text{LiNi}_x\text{Co}_y\text{Al}_{1-x-y}\text{O}_2$ , (NCA)<sup>4</sup> and  $\text{LiFePO}_4$  (LFP)<sup>5</sup> for pulsed at high rate. For the LFP cells tested at 15C discharge rate, the rapid cell capacity decay was attributed to the increase in cell resistance and not the loss of active material.

Cell degradation theory and prediction is critically important to multiple commercial applications and is an active area of research. Models have been proposed based on empirical<sup>6</sup> and physics based aging mechanisms.<sup>7,8</sup>

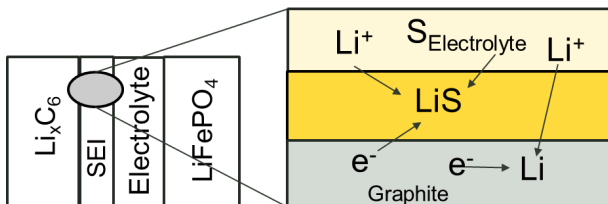


Figure 2 The desired electrochemical reaction is the lithium intercalation in graphite, but lithium can also react with components of the electrolyte to form a solid-electrolyte interphase.

Based on previous work, the cell degrades due to the consumption of active Li material via solid

electrolyte interphase (SEI) growth<sup>9</sup> as shown in Figure 2.

## 3. Experimental

Based on the use of LFP cells in commercial pulse power applications such as power tools and long life time, a 26650 LFP cell was selected. The cell properties are shown in Table 1.

Table 1 26650 LFP Cell

Description	Value
Nominal Capacity	2.3 Ah
Nominal Voltage	3.3 V
Maximum Pulse Discharge	120 A
Cycle life at 10C/ 100% DOD	1000 cycles
Cut Off Voltage	2.0 V
Cell weight	70 g

The cells were attached to an A&D / BITRODE electronic load with thermocouples affixed to the cell negative tab and cell skin surface. The cells were then placed into a thermal chamber for environmental control at 10°C for automated lifetime testing. The test schedule is shown in Table 2.

Table 2 LFP Pulse schedule

Step	Description
1	10 A charge to 100% SOC / 3.6 V
2	120 A for $t$ seconds, followed by 8 s cooling
3	Step (2) repeats until 0% SOC / 2.0 V
4	Temperature and Capacity measured
5	Return to Step (1)

## 4. Results

Figure 3 shows the cell's voltage and current response to a load profile as shown in Table 2 with a 120 A pulse for 2s. It can be seen the cell can sustain the pulse for 6 minutes before it reaches the 2V discharge limit. It is then charged for 13 minutes before it reaches 3.6V / 4A limit. The initial capacity with this profile was 1.84 Ah. The cell under a 120A pulse for 3s, shows a similar profile, with an initial capacity of 1.95 Ah.

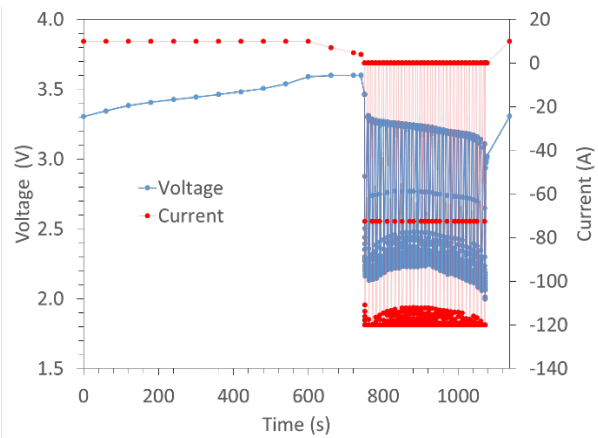


Figure 3 Current and Voltage Characteristics of LFP 2.3 Ah under test during charge and discharge

As shown in Figure 4, the heat generation due to the 3s 120A pulse increases the cell skin temperature to 58°C. This is significantly higher than the 41°C maximum observed during the 2s pulse profile. Both cells cool during the charge profile due to the 10°C ambient air cooling.

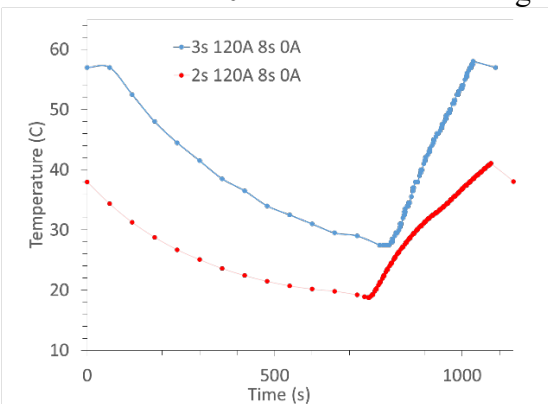


Figure 4 Temperature characteristics of test during charge and discharge. Heating occurs during discharge at 120 A pulses. Cooling occurs during charge at 10 A. Ambient temperature is 10 °C.

The degradation data is shown in Figure 5, where capacity loss is based on initial cycle capacity during the pulse profile. The 3s 120A pulse shows higher degradation (32%) than the 2s 120 A pulse (22%) after 250 cycles. The degradation is substantial higher than the expected degradation (1000 cycles), which may occur due to higher temperature.

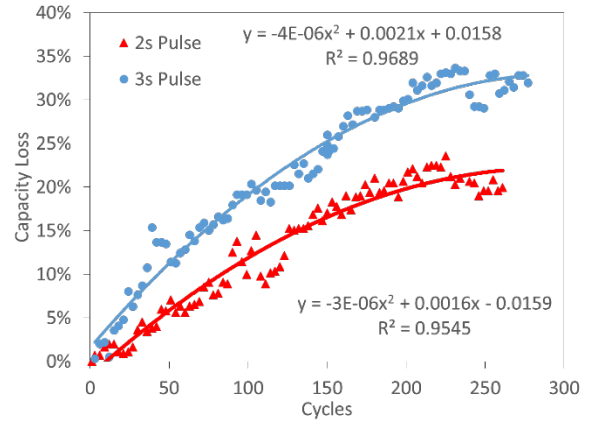


Figure 5 LFP 2.3 Ah cell capacity loss with 120 A pulsing for 2s and 3s. The degradation is significantly lower than 1000 cycle design target

## 5. Discussion

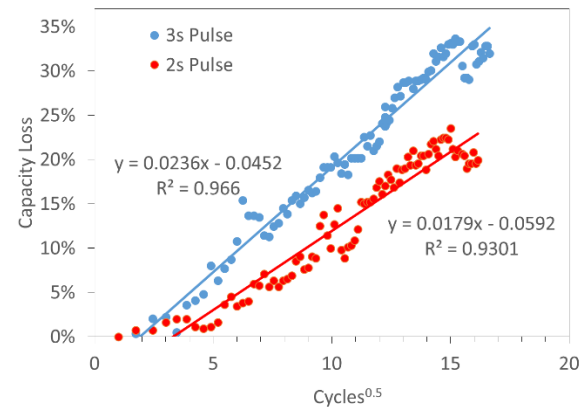


Figure 6 2.3 Ah cell capacity loss vs  $t^{0.5}$ . The degradation trend line suggests the dominant degradation is SEI growth consuming active material (Li)

Based on previous work<sup>10,11</sup> the dominant degradation mechanism is SEI growth by consumption of active material, *i.e.*, Li.

Assuming that capacity loss ( $Q_{loss}$ ) is based on the SEI consumption of lithium ( $J_{SEI}$ ):

$$Q_{loss} = \int_{t_0}^t J_{SEI} dt \quad \text{Eq.1}$$

And assuming that the SEI thickness ( $s$ ) growth is first order in lithium concentration<sup>11</sup>:

$$\frac{ds}{dt} = \frac{J_{SEI} m_{massSEI}}{\rho_{ASEI}} = \frac{k D_{Li} C^0}{1+k s} \quad \text{Eq. 2}$$

Where is  $C^0$  the bulk electrolyte concentration,  $D_{Li}$  is the diffusion coefficient and  $k$  is the rate constant. It can be shown for large time<sup>11</sup>:

$$Q_{loss} = K_1\sqrt{t} - K_2 \quad \text{Eq.3}$$

with  $K_1, K_2$  as fitting constants. Thus if SEI growth is dominating capacity loss, a plot of capacity loss vs.  $\sqrt{t}$  should be linear. This is shown in Figure 5, suggesting SEI growth causes the observed degradation.

## 6. Conclusion

Based on pulsed discharge, accelerated degradation was observed on LFP cells. The degradation increased based on the duration of the pulse, potentially due to the higher temperature observed due to increased joule heating. Based on preliminary analysis, it appears that lithium loss due to SEI growth is dominant loss mechanism. Future work involves model development to predict failure at different conditions and additional cell characterization techniques to further elucidate degradation mechanisms and identify mitigation measures.

## 1. REFERENCES

[1] Ed Mazzanti, MG R. M. Dyess, ARCIC, US ARMY October, 2017

[2] D. Erb, PhD Thesis, Massachusetts Institute of Technology 2016  
 [3] J. Nairus, et al DOD Energy & Power S&T Roadmap, September, 2017  
 [4] D. Wong, B Shrestha, D Wetz, J Heinzl, J. Power Sources, 363-372 (280), 2015  
 [5] D. Wong, D. Wetz, J. Heinzl, A. Mansour, J. Power Sources 81-90 (328), 2016  
 [6] J. Wang, P. Liu, J. Hicks-Garner, E. Sherman, S. Soukiaziana, M. Verbrugge, H. Tatariab, J. Musser, P. Finamore, J. Power Sources 3942–3948(196), 2011  
 [7] M. Schimpe, M. E. von Kuepach, M. Naumann, H. C. Hesse, K. Smith, and A. Jossen, J. Electrochemical Soc., A181-A193 165 (2) 2018  
 [8] R. Deshpande and D Bernardi, J. Electrochemical Soc., A461-A474 164 (2) 2017  
 [9] E. Peled and S. Menkin, J. Electrochemical Soc., A1703-A1719 164 (7) 2017  
 [10] M. Broussely, S. Herreyre, P. Biensan, P. Kasztejna, K. Nechev and R.J. Staniewicz, J. Power Sources 13-21 (97-98) 2001  
 [11] M. B. Pinson and M. Bazant, J Electrochem. Soc., A243-A250 160 (2), 2013